Blockage Attenuation and Duration Over Reflected Propagation Paths in Indoor Terahertz Deployments

Anatoliy Prikhodko[1,2], Abdukodir Khakimov[3], Evgeny Mokrov[3], Vyacheslav Begishev[3(✉)], Alexander Shurakov[1,2], and Gregory Gol'tsman[1,2]

[1] Moscow Pedagogical State University, Moscow, Russia
anprihodko@hse.ru, {alexander,goltsman}@rplab.ru
[2] National Research University Higher School of Economics, Moscow, Russia
[3] Peoples' Friendship University of Russia (RUDN University), Moscow, Russia
{khakimov-aa,mokrov-ev,begishev-vo}@rudn.ru

Abstract. The future 6G cellular systems are expected to utilize the lower part of the terahertz frequency band, 100–300 GHz. As a result of high path losses, the coverage of such systems will be limited to a few tens of meters making them suitable for indoor environments. As compared to outdoor deployments, indoor usage of THz systems is characterized by the need to operate over shorter distances using the reflected propagation paths. This paper aims to characterize the impact of blockage of reflected propagation paths in typical scenarios. Specifically, we carry out a detailed measurements campaign at 156 GHz and report reflection losses, blockage losses over the reflected path as well as blockage duration, signal fall and rise times. Our results show that signal polarization has a profound impact on the reflection losses with E-plane horizontally oriented signal losses being at least 8 dB higher as compared to H-plane signal horizontal orientation. Furthermore, the reflection material types do not affect the mean blockage attenuation over the reflected paths. Generally, the presence of a reflector neither quantitatively nor qualitative changes the mean attenuation induced by a blockage phenomenon.

Keywords: 6G · terahertz · reflections · blockage · attenuation · duration · signal fall · rise times

1 Introduction

Seeking for the capacity boost at the access interface in cellular systems, ITU-R and 3GPP utilize millimeter wave (mmWave) bands, 30–100 GHz for 5G New

This study was conducted as a part of strategic project "Digital Transformation: Technologies, Effectiveness, Efficiency" of Higher School of Economics development programme granted by Ministry of science and higher education of Russia "Priority-2030" grant as a part of "Science and Universities" national project. Support from the Basic Research Program of the National Research University Higher School of Economics is gratefully acknowledged.

V. M. Vishnevskiy et al. (Eds.): DCCN 2023, LNCS 14123, pp. 423–434, 2024.
https://doi.org/10.1007/978-3-031-50482-2_33

Radio (NR) systems [11,14]. The next step in the evolution of such systems is the utilization of the lower part of the terahertz (THz) frequency band, where large parts of the spectrum are still not regulated and tens of gigahertz of bandwidth can be allocated to 6G systems [5,9].

To partially compensate for the reduction in the effective antenna aperture that reduces with the increase of the carrier frequency, similarly to 5G NR mmWave systems, 6G sub-THz systems will heavily rely upon the use of antenna arrays at both base station (BS) and user equipment (UE) operating in beamforming mode [10]. Nevertheless, the coverage of such systems will still be limited to tens or hundreds of meters making them a suitable choice for indoor areas, where most of the traffic demands originate. The landscape of applications in the indoor environment is rather large including conventional 4k/8k video watching, virtual/augmented reality (AR/VR) gaming, and forthcoming applications such as collective VR gaming, holographic communications [6], etc.

Indoor deployments of 6G sub-THz systems are characterized by several propagation specifics. First of all, the link distances are on average smaller as compared to those outdoors. Secondly, due to rather small heights of BS, human body blockage is more likely to occur. Finally, as a result of the complex geometry of indoor premises, communications over reflected paths are expected to be much more common. Specifically, short distances have been recently shown to lead to much smaller human body blockage attenuation at 156 GHz varying in the range of $8-13$ dB [12] as compared to 15–35 dB losses over larger distances and at lower frequencies, e.g., as reported in [4,7].

The aim of this paper is to characterize reflected propagation paths in indoor environments in the sub-THz frequency band. Specifically, by carrying out a large-scale measurement campaign at carrier frequency of 156 GHz, we characterize reflection losses of different materials and blockage attenuation of reflected propagation paths. In addition to attenuation, we also investigate time-related metrics such as blockage duration as well as signal rise and fall times. The main findings of our paper acquired empirically are:

- the orientation of the antenna polarization plane has a profound impact on the reflection losses with horizontally oriented polarization plane losses being at least 7 dB higher as compared to vertically orientated polarization plane;
- the reflection material types do not affect the mean blockage attenuation over the reflected paths;
- the presence of reflector neither quantitatively nor qualitative changes the mean attenuation induced by a blockage phenomenon;
- blockage, fall and rise times for drywall are characterized by slightly smaller mean values as compared to concrete for vertical polarization plane.

The paper is organized as follows. First, in Sect. 2, we overview related studies reported in the literature. Next, in Sect. 3, we outline experimental setup. The main results of the conducted experiments are reported further in Sect. 4. And conclusions are provided in the last section.

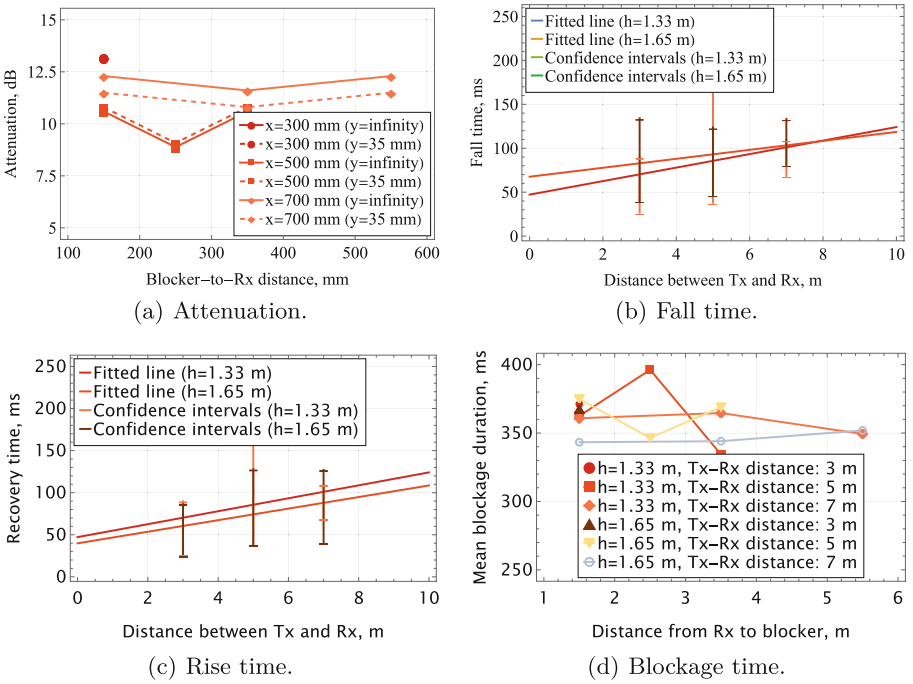

(a) Attenuation. (b) Fall time.

(c) Rise time. (d) Blockage time.

Fig. 1. Mean attenuation, mean signal blockage, fall and rise times

2 Related Work

In this section, we outline related works. We start by briefly reminding the results for non-reflected path propagation and blockage. They are recapitulated for comparison purposes in our study. Then, we discuss results similar to those reported in our study which are related to reflection losses and blockage of reflected propagation paths in the mmWave and THz bands.

As one of the paper goals is to compare blockage statistics over reflected paths to that over primary line-of-sight (LoS) paths, we briefly introduce the latter as reported earlier in [12]. To this aim, Fig. 1 provides mean attenuation, mean signal blockage, fall and rise times for different Tx-to-Rx distances, x, LoS heights, h, and Rx-to-blocker distances. By analyzing the presented results, one may observe that the mean attenuation varies between 8–13 dB and is generally independent of blocker-to-Rx and Tx-to-Rx distances. Furthermore, both fall and rise times increase as a function of the distance potentially making it more feasible to detect blockage events timely. The absolute difference between the reported times is insignificant and lies within 2–4% of the nominal value (e.g., 60 ms for $x = 3$ m, 80 ms for $x = 5$ m and 100 ms for $x = 7$ m for fall times). It is worth noting that both fall and rise times have almost identical nominal values, and, in general, the rise time is 7–10% smaller than the fall time.

The attenuation caused by reflections from different materials was the subject of several studies. In [3], the authors reported the measurement results of the received signal reflected from aluminum, glass, plastic, hardboard and concrete using THz time-domain spectroscopy (THz-TDS) equipment for different angles of incidence. The time duration of utilized pulses was chosen such that the energy is mainly concentrated in the 0.1–4 THz band. The observed losses were in the range of 10–60 dB depending on the angle of incidence and type of the material. Specifically, in the 0.1–0.3 THz band, aluminum demonstrated the least attenuation of around 25–35 dB for the angle of incidence of $\pi/4$. The rest of the materials provided higher attenuation.

The authors in [1,8] reported the results of reflections from typical vehicle materials at 300 GHz for different configurations including front and rear reflections, side-lane and under-vehicle reflections. The front and rear reflections were reported to result in 24–42 dB and 15–30 dB attenuations, respectively, while side-lane reflections led to additional 16–20 dB losses. The authors also proposed to model the under-vehicle reflection losses of the asphalt by utilizing the $\alpha d^{-\beta}$ function, where d is the separation distances, while α and β are some coefficients tabulated in Table 1 in their manuscript.

Similar studies have been performed in the mmWave band. In [2], specifically, the authors investigated the impact of polarization properties of the indoor 38 GHz channel after single bounce reflection for different angles of incidence and observation and two types of materials: aluminum and concrete. They highlighted that, when the polarization of Tx and Rx antennas coincide, much smaller losses are experienced. The difference can reach 15–20 dB and is maximized for peculiar reflections. Concrete results in 8–12 dB higher losses as compared to aluminum.

3 Experimental Setup

In this section, we introduce our measurement setup and present details on the acquisition of experimental data.

A schematic of the measurement setup employed for blockage studies is presented in Fig. 2a. We use a 156 GHz constant waveform source with amplitude modulation at 25 kHz. It provides a 6° wide beam incident on the material under test (MUT) at a constant angle of 70°. The reflected beam is received by a low-barrier diode detector equipped with the same optics as the source. A lock-in amplifier is used to readout the detector response voltage. When a blocker walks across the reflected beam at the midpoint between MUT and the detector, the voltage-vs-time series is registered by a digital signal oscilloscope (DSO). The measurement covers a time frame of 4 s with a resolution of 100 μs. Referring to Fig. 2a, list of the employed measurement equipment includes the following items:

- microwave synthesizer: Hittite HMC-T2220;
- frequency multiplier: RPG Tx-134-158-20;
- ultrafast switch: ELVA-1 VCVA-06;

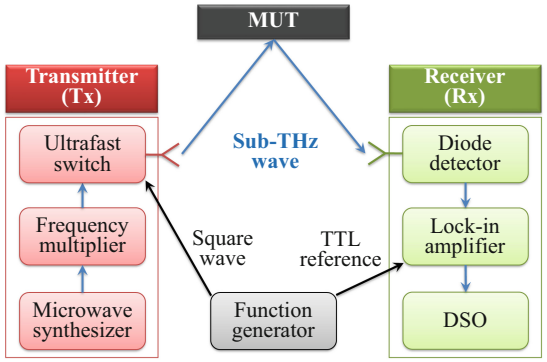

(a) Measurement equipment.

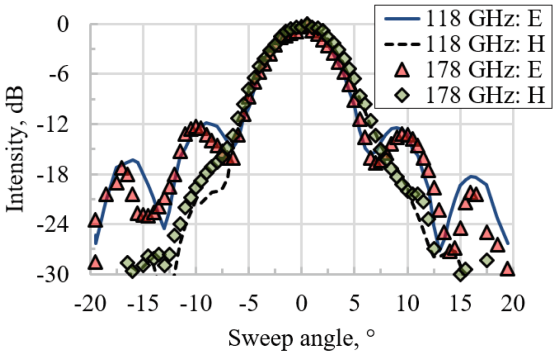

(b) Tx/Rx radiation pattern.

Fig. 2. Experimental setup

– function generator: SRS DS345;
– diode detector: DOK WR-06;
– lock-in amplifier: SRS SR844;
– DSO: R&S RTO1012.

The source-to-detector (Tx-to-Rx) optical path of 3 m is chosen in all the measurements. The source provides 52 mW of power, and the setup ensures a signal-to-noise ratio of up to 3×10^4 at the detector output. Measured response voltages are further converted into power levels at the detector input via its responsivity, which is equal to 500 V/W at 156 GHz. MUT is successively presented by concrete, drywall and class samples with thicknesses of 50, 12.5 and 6 mm, respectively. The sample linear dimensions of 0.5 m × 0.5 m are chosen to overlap a 156 GHz beam upon reflection. The sample is installed in a wooden frame to set its center at 1.65 m above the floor which corresponds to the LoS height between the source and the detector. Spurious reflections from the wall behind the sample are geometrically filtered out by the positioning of the measurement equipment. Input optics of the source and the detector rely on a pyra-

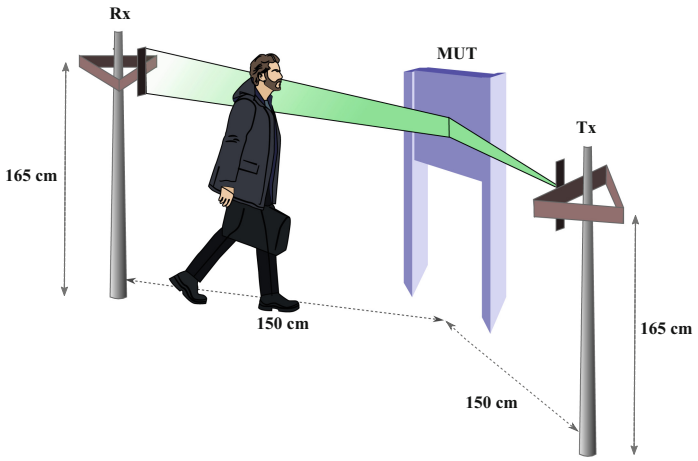

Fig. 3. Illustration of the considered scenario

midal horn known as a wide-band antenna with different side lobe levels in H- and E-planes, see Fig. 2b. We make use of this feature and conduct a series of measurements for two orientations of the horn antennas, when either their H- or E-planes are horizontally oriented, i.e., coinciding with the plane of incidence of the transmitted 156 GHz beam.

The schematic illustration of the scenario is shown in Fig. 3.

4 Measurements Results

In this section, we report our results. We start with visual illustrations of the blockage phenomenon over the reflected paths. Then, we characterize the mean attenuation caused by reflection for typical types of wall materials such as drywall, concrete and glass. Further, we investigate blockage attenuation over reflected paths. Finally, we report mean and cumulative distribution function (CDF) of blockage duration, signal fall and rise times for reflected paths.

4.1 Time Series

We start with a time series representation of the blockage over the reflected paths, as demonstrated in Fig. 4, for all the considered types of materials and orientations of the Tx/Rx antennas. Here, for comparison purposes, we also demonstrate blockage over the LoS path ("direct trace" in Fig. 4).

By visually inspecting the presented data, one may notice that the received signal level in no blockage condition is significantly lower as compared to direct LoS propagation. This is attributed to the reflection losses considered in details below. Furthermore, we observe significant difference between signal levels and blockage profiles for horizontally and vertically oriented E-planes of Tx/Rx

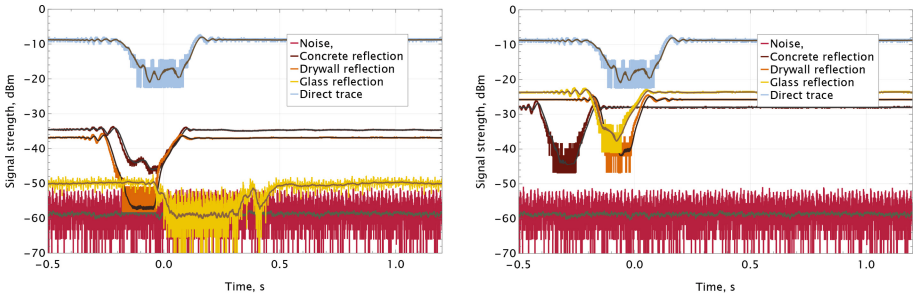

(a) Horizontal plane. (b) Vertical plane.

Fig. 4. Comparison of reflection and direct traces

antennas (the H-planes are respectively orthogonal). The former condition is referred to as horizontal plane (HP), and the latter – as vertical plane (VP). Specifically, we see that the signal strength for the HP reflection from glass is barely higher than the noise level. And for the VP reflection case, it is comparable to other materials. Finally, visual inspection does not allow clearly highlight any difference between attenuation- and time-related blockage profiles for different materials requiring detailed statistical analysis.

4.2 The Impact of Reflection

We start our analysis with the characterization of the reflection losses by comparing the reflected signal against the LoS signal studied earlier in [12]. In order to determine reflection losses, we utilize the propagation model, $L(x)$, with the coefficients y_1 and y_2 empirically derived from the signal difference between Tx and Rx at different distances.

$$L(x) = y_1 \log_{10} x + 20 \log_{10} f_c + y_2 + I_B L_B(x, d), \tag{1}$$

In the case of LoS propagation for the carrier frequency of 156 GHz, the coefficients are $y_1 = -22.04$ and $y_2 = -251.704$ [12].

By utilizing (1), we subtract the model's values from the path losses observed in non-LoS conditions obtaining the reflection losses. These losses are reported in Table 1 for different types of materials and polarizations. By analyzing the presented data, one may deduce that the impact of the polarization plane orientation is critical. For the VP condition, all the materials behave similarly leading to 14–19 dB losses with glass having 4 dB gain on top of concrete. The HP condition, however, is characterized by at least 7–13 dB stronger attenuations. Specifically, there are 7 dB higher losses for concrete and 11 dB higher losses for drywall. In the HP condition, glass attenuates the signal on reflection by approximately 42 dB making the reflected path signal strength comparable to noise, see Fig. 4. We specifically note that attenuation of at least 30 dB may lead to the loss of connectivity depending on the propagation distance between Tx and Rx.

4.3 Blockage Attenuation Over Reflected Paths

Now, we proceed to characterize the blockage attenuation over the reflected paths. To this aim, we subtract the value of the received signal with no blockage impairments from the average value in the blocked state. Table 2 presents the mean blockage attenuation and the mean values of the signal strength propagated directly to the Tx and reflected from the considered materials in blocked and non-blocked cases.

By analyzing the reported data, one may observe that, while the antenna polarization plane orientation greatly impacts on the received signal strength, the impact on the mean blockage value is rather limited. All the material types lead to almost constant blockage attenuation of approximately 9–10 dB for the VP orientation. By comparing the obtained results with those reported in Fig. 1 for non-reflected blockage, one may deduce that the presence of a reflector neither quantitatively nor qualitatively changes the mean attenuation induced by a human blockage phenomenon. The HP orientation is characterized by larger differences between mean blockage attenuations varying in the range of 7–10 dB. However, these changes can be potentially attributed to smaller signal strengths accompanied by reduction in measurement accuracy for drywall and glass.

To provide additional information regarding the attenuation, Fig. 5 reports cumulative distribution functions (CDFs) of blockage attenuations for concrete and drywall materials. The illustration highlights the difference between blockages for different orientations of the antenna polarization plane. Notably, the range of attenuation can be quite large varying between approximately 6 and 10 dB. These differences can be attributed to slight changes in the trajectory of a person crossing the LoS path.

4.4 Fall, Rise and Blockage Times

In addition to attenuation statistics, time-related parameters of blockage are of importance for the design of sub-THz communications systems. In this section, we report blockage, fall and rise times including their mean values and CDFs. Note that the rise time is of special importance in the context of blockage

Table 1. Reflection and blockage losses

Type	Reflection loss, dB	Blockage loss, dB
Concrete, HP	25.85	33.84
Drywall, HP	27.97	37.96
Glass, HP	41.59	48.08
Concrete, VP	18.93	28.76
Drywall, VP	16.87	25.94
Glass, VP	14.79	23.60

Table 2. The mean blockage attenuation

Type	Signal, dBm	Blocked signal, dBm	Blockage attenuation, dB
Direct, LoS	–8.88	–16.21	7.32
Concrete, HP	–34.74	–42.73	7.98
Drywall, HP	–36.86	–46.85	9.99
Glass, HP	–50.48	–56.97	6.48
Concrete, VP	–27.82	–37.65	9.83
Drywall, VP	–25.76	–34.83	9.07
Glass, VP	–23.68	–32.48	8.80

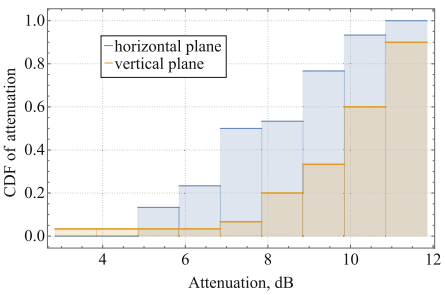

(a) Concrete.

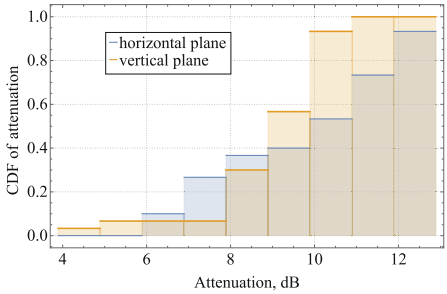

(b) Drywall.

Fig. 5. CDFs of blockage attenuation for concrete and drywall

detection [12,13], while the blockage time is critical for designing algorithms to improve service reliability.

The mean values of the considered metrics are summarized in Table 3. By analyzing the reported values, one may observe that there is a 8% difference between blockage times for concrete and drywall for the VP antenna orientation. Mean rise time for drywall is 30% smaller than for concrete, and their fall times are almost identical. Note that for the HP orientation, all these values differ by 5–8% as evident from Table 3. Still, recalling the results for blockage remedies, these

Table 3. Mean fall, rise and blockage times

Type	Blockage time, ms	Rise time, ms	Fall time, ms
Concrete, HP	316	101	61
Drywall, HP	333	94	66
Concrete, VP	308	92	90
Drywall, VP	285	71	89

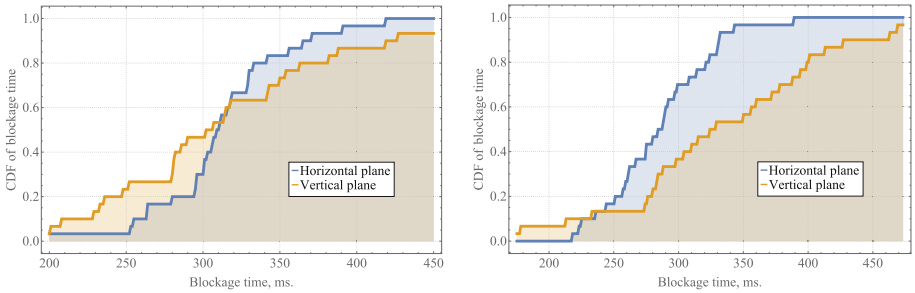

(a) Concrete. (b) Drywall.

Fig. 6. CDF of blockage times

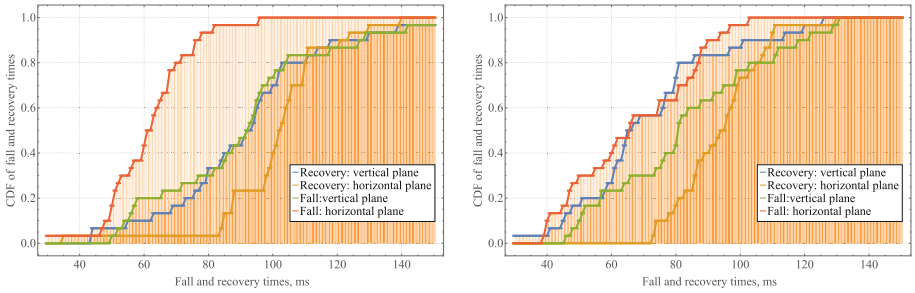

(a) Concrete. (b) Drywall.

Fig. 7. CDFs of fall and rise times

deviations are expected to not affect the design of blockage detection algorithms [12,13].

Complementing the mean values, we present the CDFs of blockage, fall and rise times in Fig. 6 and 7. The blockage duration CDFs indicate that CDF for concrete is steeper as compared to drywall and also has a smaller range of approximately 200 ms. Also, the VP antenna orientation leads to a noticeably smoother increase in CDF behavior. In practice, it means that deviation in blockage duration for the HP antenna orientation is much more clustered around its mean-making.

By analyzing CDFs of fall and rise times demonstrated in Fig. 7, one may observe that drywall is characterized by a slightly wider range of values as compared to concrete. The difference in these times for different orientations of the antenna polarization plane is also noticeable. This generally means that the time budget for the detection of blockage events is higher for drywall.

5 Conclusions

As most of the traffic in cellular systems originates indoors, where the link distances are generally shorter while communications over reflected paths are more

common as compared to outdoor deployments, in this paper, we performed a measurements campaign at 156 GHz characterizing the reflection and blockage losses of reflected paths. We considered different types of reflection materials typical for the indoor environment including concrete, drywall and glass.

Our main findings are: (i) the orientation of the antenna polarization plane has a profound impact on the reflection losses with horizontally oriented polarization plane losses being at least 7 dB higher as compared to vertically orientated polarization plane, (ii) the reflection material types do not affect the mean blockage attenuation over the reflected paths, (iii) the presence of reflector neither quantitatively nor qualitative changes the mean attenuation induced by a blockage phenomenon, (iv) blockage, fall and rise times for drywall are characterized by slightly smaller mean values as compared to concrete for vertical polarization planes. In general, blockage statistics over reflected paths are similar to that for LoS paths and do not require special communications algorithms design.

Acknowledgements. This study was conducted as a part of strategic project "Digital Transformation: Technologies, Effectiveness, Efficiency" of Higher School of Economics development programme granted by Ministry of science and higher education of Russia "Priority-2030" grant as a part of "Science and Universities" national project. Support from the Basic Research Program of the National Research University Higher School of Economics is gratefully acknowledged.

References

1. Eckhardt, J.M., Petrov, V., Moltchanov, D., Koucheryavy, Y., Kürner, T.: Channel measurements and modeling for low-terahertz band vehicular communications. IEEE J. Sel. Areas Commun. **39**(6), 1590–1603 (2021)
2. Gaspard, I.: Co-and crosspolar scattering measurements at slightly rough walls for indoor propagation channels at mmwaves. In: 2019 IEEE-APS Topical Conference on Antennas and Propagation in Wireless Communications (APWC), pp. 038–041 (2019). https://doi.org/10.1109/APWC.2019.8870411
3. Kokkoniemi, J., Petrov, V., Moltchanov, D., Lehtomäki, J., Koucheryavy, Y., Juntti, M.: Wideband terahertz band reflection and diffuse scattering measurements for beyond 5G indoor wireless networks. In: European Wireless 2016; 22th European Wireless Conference, pp. 1–6. VDE (2016)
4. MacCartney, G.R., Rappaport, T.S., Rangan, S.: Rapid fading due to human blockage in pedestrian crowds at 5g millimeter-wave frequencies. In: GLOBECOM 2017–2017 IEEE Global Communications Conference, pp. 1–7. IEEE (2017)
5. Matthaiou, M., Yurduseven, O., Ngo, H.Q., Morales-Jimenez, D., Cotton, S.L., Fusco, V.F.: The road to 6G: ten physical layer challenges for communications engineers. IEEE Commun. Mag. **59**(1), 64–69 (2021)
6. Moltchanov, D., Sopin, E., Begishev, V., Samuylov, A., Koucheryavy, Y., Samouylov, K.: A tutorial on mathematical modeling of 5G/6G millimeter wave and terahertz cellular systems. IEEE Commun. Surveys Tutor. **24**, 1072–1116 (2022)
7. Nie, S., MacCartney, G.R., Sun, S., Rappaport, T.S.: 72 GHz millimeter wave indoor measurements for wireless and backhaul communications. In: 2013 IEEE

24th Annual International Symposium on Personal, Indoor, and Mobile Radio Communications (PIMRC), pp. 2429–2433. IEEE (2013)
8. Petrov, V., Eckhardt, J.M., Moltchanov, D., Koucheryavy, Y., Kurner, T.: Measurements of reflection and penetration losses in low terahertz band vehicular communications. In: 2020 14th European Conference on Antennas and Propagation (EuCAP), pp. 1–5. IEEE (2020)
9. Petrov, V., Pyattaev, A., Moltchanov, D., Koucheryavy, Y.: Terahertz band communications: applications, research challenges, and standardization activities. In: 2016 8th International Congress on Ultra Modern Telecommunications and Control Systems and Workshops (ICUMT), pp. 183–190. IEEE (2016)
10. Roh, W., et al.: Millimeter-wave beamforming as an enabling technology for 5g cellular communications: theoretical feasibility and prototype results. IEEE Commun. Mag. **52**(2), 106–113 (2014)
11. Shafi, M., et al.: 5g: a tutorial overview of standards, trials, challenges, deployment, and practice. IEEE J. Sel. Areas Commun. **35**(6), 1201–1221 (2017)
12. Shurakov, A., et al.: Empirical blockage characterization and detection in indoor sub-thz communications. Comput. Commun. **201**, 48–58 (2023)
13. Wu, S., Alrabeiah, M., Hredzak, A., Chakrabarti, C., Alkhateeb, A.: Deep learning for moving blockage prediction using real mmwave measurements. In: ICC 2022-IEEE International Conference on Communications, pp. 3753–3758. IEEE (2022)
14. Zaidi, A., Athley, F., Medbo, J., Gustavsson, U., Durisi, G., Chen, X.: 5G Physical Layer: Principles, Models and Technology Components. Academic Press, Cambridge (2018)